PHYSICAL REVIEW B **78**, 020510(R) (2008)

Edge-type Josephson junctions in narrow thin-film strips

Maayan Moshe,[1] V. G. Kogan,[2] and R. G. Mints[1,*]
[1]*The Raymond and Beverly Sackler School of Physics and Astronomy, Tel Aviv University, Tel Aviv 69978, Israel*
[2]*Ames Laboratory - DOE and Department of Physics and Astronomy, Iowa State University, Ames, Iowa 50011, USA*
(Received 1 July 2008; published 23 July 2008)

We study the field dependence of the maximum current $I_m(H)$ in narrow edge-type thin-film Josephson junctions. We calculate $I_m(H)$ within nonlocal Josephson electrodynamics taking into account the stray fields. These fields affect the difference of phases of the order parameter across the junction and therefore the tunneling currents. We find that the phase difference along the junction is proportional to the applied field, depends on the junction geometry, but is independent of the Josephson critical current density, i.e., it is universal. An explicit formula for this universal function is derived and used to calculate $I_m(H)$. It is shown that the maxima of $I_m(H) \propto 1/\sqrt{H}$ and the zeros of $I_m(H)$ are equidistant only in high fields. We find that the spacing between the zeros is proportional to $1/w^2$, where w is the width of the junction. The general approach is applied to calculate $I_m(H)$ for a superconducting quantum interference device (SQUID) with two narrow edge-type junctions.

DOI: 10.1103/PhysRevB.78.020510 PACS number(s): 74.50.+r

Physics of the edge-type thin-film Josephson junctions (two films in the (x,y) plane touching only along the edges at $x=0$ with no overlap as shown in Fig. 1) differs significantly from that of the junctions with bulk banks. The main reason for this difference is the effect of the stray fields on the tunneling currents in the junction and on the screening currents in its banks. As a result, the phase difference across the junction, $\varphi(y)$, is described by an integral equation, i.e., the Josephson electrodynamics of edge-type thin-film junctions is *nonlocal*.[1–5]

Development of the nonlocal electrodynamics of these junctions is still in progress and is a subject of growing theoretical and experimental interest.[6–9] In particular, it was shown that the nonlocality caused by the stray fields slows down the electromagnetic waves propagating along the junction.[3] This effect leads to an interesting and important result—Cherenkov radiation by fast moving Josephson vortices.[3,9] The features of the edge-type junctions such as large I_cR products and low noise are attractive for applications.[10]

Nonlocality caused by the long-range stray fields is especially important for physics of series of interchanging 0- and π-shifted junctions.[6–8] If the length scale of the 0- and π-shifted fragments is much less than the Josephson length, these systems behave as anomalous Josephson junctions with critical current density alternating along the junction. This anomaly results in appearance of spontaneous flux, splinter vortices carrying nonquantized flux, and peculiar dependencies of the maximum current $I_m(H)$ on the applied field. These effects have been studied in asymmetric grain boundaries in thin YBCO films, superconductor-ferromagnet-superconductor, superconductor-insulator-ferromagnet-superconductor heterostructures, and YBCO/Nb zigzag junctions.[6–8,11–16]

The phase distribution $\varphi(y)$ along edge-type thin-film junctions ($\lambda \gg d$) has an intrinsic length scale,

$$\ell = c\phi_0/8\pi^2\Lambda g_c, \tag{1}$$

where g_c is the critical sheet current density of the junction, $\Lambda = 2\lambda^2/d$ is the Pearl length, λ is the London penetration depth, and d is the film thickness (we call ℓ the thin-film Josephson length, although in long junctions the vortex size is $\sim\sqrt{\ell\Lambda}$). We show that if the width w of the strip is shorter than ℓ and Λ, then $\varphi(y)$ is ℓ independent, i.e., the same for junctions with different Josephson critical currents.[17] Thus, for narrow junctions ($w \ll \Lambda$ and $w \ll \ell$), $\varphi(y)$ is a *material independent universal* function; it depends only on the applied field and the junction length.[18]

In this Rapid Communication we evaluate the field dependence of the maximum supercurrent $I_m(H)$ through the junction that turns out to be quite different from the standard Fraunhofer pattern of bulk junctions. Zeros of $I_m(H)$ become equidistant only in large fields, and are separated by $\Delta H \sim \phi_0/w^2$, which typically is much smaller than $\phi_0/w\lambda$ of bulk junctions of the same length. The maxima of $I_m(H)$ decrease as $1/\sqrt{H}$, which is slower than $1/H$ for the bulk. The approach developed is applied to calculate $I_m(H)$ for a superconducting quantum interference device (SQUID) made of narrow thin-film strips with edge-type junctions and to show that $I_m(H)$ differs remarkably from the canonic Fraunhofer pattern.

The sheet current density $\boldsymbol{g}=(g_x,g_y)$ in thin films can always be written as $\boldsymbol{g}=\mathrm{curl}\, S\hat{z}=(\partial_y S,-\partial_x S)$, where $S(x,y)$ is the stream function. The sheet current normal to the strip edges ($y=\pm w/2$) is zero, i.e., $S(x,\pm w/2)$ are constants. The total current I through the strip is

$$I = \int_{-w/2}^{w/2} g_x dy = S(w/2) - S(-w/2). \tag{2}$$

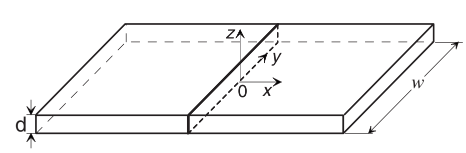

FIG. 1. Sketch of an edge-type thin-film Josephson junction. The junction plane is shown by the dotted cross section.

Integrating London equations over the film thickness we obtain

$$h_z + \frac{2\pi\Lambda}{c}\mathrm{curl}_z\boldsymbol{g} = \frac{\phi_0}{2\pi}\delta(x)\varphi'(y), \tag{3}$$

where h_z consists of the applied field H and the part related to $\boldsymbol{g}$ by the Biot-Savart integral. The right-hand side here is a manifestation of a general rule: The field of a Josephson junction is formally equivalent to the field of a set of vortex-like singularities distributed along the junction with the line density $\varphi'(y)/2\pi$.[2,5]

In strips with $w \ll \Lambda$, the self-field of the current $\boldsymbol{g}$ is of the order g/c, whereas the second term on the left-hand side of Eq. (3) is of the order $g\Lambda/cw \gg g/c$. Hence, the self-field can be disregarded, unlike the *applied* field H. Substituting $\mathrm{curl}_z\boldsymbol{g} = -\nabla^2 S$ in Eq. (3), one obtains

$$\frac{2\pi\Lambda}{c}\nabla^2 S = -\frac{\phi_0}{2\pi}\delta(x)\varphi'(y) + H. \tag{4}$$

This *linear* equation has solutions $S = S_1 + S_2$ such that

$$\frac{2\pi\Lambda}{c}\nabla^2 S_1 = -\frac{\phi_0}{2\pi}\delta(x)\varphi'(y), \quad \frac{2\pi\Lambda}{c}\nabla^2 S_2 = H. \tag{5}$$

The boundary condition (2) is satisfied if we assume that $S_1(\pm w/2) = 0$, $S_2(w/2) - S_2(-w/2) = I$ and

$$S_1(\boldsymbol{r}) = \int d\boldsymbol{\rho}\,\delta(u)\frac{\varphi'(v)}{2\pi}G(\boldsymbol{r},\boldsymbol{\rho}), \tag{6}$$

$$S_2(\boldsymbol{r}) = \frac{cH}{4\pi\Lambda}\left(y^2 - \frac{w^2}{4}\right) + \frac{I}{w}\left(y + \frac{w}{2}\right), \tag{7}$$

where $\boldsymbol{r} = (x,y)$ and $\boldsymbol{\rho} = (u,v)$. The Green's function $G(\boldsymbol{r},\boldsymbol{\rho})$ satisfying $(2\pi\Lambda/c\phi_0)\nabla^2 G = -\delta(\boldsymbol{r}-\boldsymbol{\rho})$ with zero boundary conditions is given by

$$G = \frac{c\phi_0}{4\pi^2\Lambda}\tanh^{-1}\frac{\cos\mu\cos\eta}{\cosh(\xi-\zeta) - \sin\mu\sin\eta}, \tag{8}$$

where $(\xi,\zeta) = (\pi x/w, \pi u/w)$, $(\eta,\mu) = (\pi y/w, \pi v/w)$ are dimensionless coordinates. $G(\boldsymbol{r},\boldsymbol{\rho})$ gives the current distribution of a single vortex at $\boldsymbol{r} = \boldsymbol{\rho}$ of an infinite strip.

Clearly, S_1 describes the current perturbation due to the junction. The first term in S_2 represents the screening currents due to the applied field, whereas the second is due to the field of a uniform transport current.

Next, we introduce the reduced field h and current i,

$$h = 4w^2 H/\phi_0, \quad i = 8\pi^2\Lambda I/c\phi_0, \tag{9}$$

and use the Josephson relation $g_x(0,y) = g_c \sin\varphi(y) = \partial_y S(0,y)$ to obtain

$$\frac{w}{\ell}\sin\varphi(\mu) = \int_{-\pi/2}^{\pi/2} d\eta\,\varphi'(\eta)\frac{\cos\eta}{\sin\eta - \sin\mu} + h\mu + i. \tag{10}$$

The boundary conditions for $\varphi(\mu)$ follow from the London equation for the sheet current $g_y(\pm 0,\mu)$. A standard calculation results in $\varphi'(\mu) \propto g_y(0,\mu)$. At the edges ($\mu = \pm\pi/2$) the current component g_y must vanish, i.e.,

$$\varphi'(\pm\pi/2) = 0. \tag{11}$$

In narrow junctions ($w \ll \Lambda$ and $w \ll \ell$), the left-hand side of Eq. (10) can be disregarded. While neglecting the term $\propto w/\ell$ we have to disregard also the transport current i; otherwise, integrating both sides of Eq. (10) over the strip does not produce identity.

The truncated Eq. (10) reveals a remarkable feature of junctions in narrow strips: The phase derivative $\varphi'(\mu)$ is proportional to the applied field, i.e., $\varphi'(\mu) = h\varphi_0'(\mu)$. The function $\varphi_0'(\mu)$ is governed by the equation

$$\int_{-\pi/2}^{\pi/2} d\eta\,\varphi_0'(\eta)\frac{\cos\eta}{\sin\mu - \sin\eta} + \mu = 0, \tag{12}$$

which does not contain any physical parameter of the junction and therefore $\varphi_0'(\mu)$ is a *universal* function.

To determine $\varphi_0'(\mu)$ we introduce variables $s = \sin\eta$ and $t = \sin\mu$ and write Eq. (12) in the form

$$B_\perp(t) = \frac{1}{2\pi}\int_{-1}^{1}\frac{J(s)ds}{t-s}, \tag{13}$$

where $B_\perp(t) = -\sin^{-1}t$, $J(s) = 2\pi\sqrt{1-s^2}(d\varphi_0/ds)$. Clearly, Eq. (13) is the Biot-Savart integral for the normal component of the "field" $B_\perp(t)$ at the surface of a strip $-1 < s < 1$ carrying the "sheet current" $J(s)$. We, therefore, have to find $J(s)$ for a given $B_\perp(t)$. However, $J(s)$ is not determined uniquely by one field component. Currents of the form $C/\sqrt{1-s^2}$ with an arbitrary constant C correspond to $B_\perp = 0$. This flexibility allows us to obtain φ_0' that satisfies condition (11):

$$\varphi_0'(\mu) = \frac{1}{\pi^2\cos\mu}\left(2 - \int_{-\pi/2}^{\pi/2}\frac{\eta\cos^2\eta\,d\eta}{\sin\mu - \sin\eta}\right). \tag{14}$$

The integral in Eq. (14) is understood as Cauchy principal value and can be done numerically. The universal function $\varphi_0'(\mu)$ so calculated is shown in Fig. 2(a). The function $\varphi_0(\mu)$ obtained requiring it to be odd in μ is shown in Fig. 2(b). In particular, this calculation gives $\varphi_0(\pi/2) - \varphi_0(-\pi/2) \approx 0.86$.

We thus obtain for any applied field in narrow thin-film junctions: $\varphi(\mu) = h\varphi_0(\mu) + \theta$ with an arbitrary θ. The total current through the junction is

$$I = \frac{g_c w}{\pi}\int_{-\pi/2}^{\pi/2} d\mu\,\sin[h\varphi_0(\mu) + \theta]. \tag{15}$$

Maximizing the value of I with respect to θ provides $\theta = \pi/2$ and the maximum current I_m:

$$\frac{I_m}{g_c w} = \frac{1}{\pi}\left|\int_{-\pi/2}^{\pi/2} d\mu\,\cos[h\varphi_0(\mu)]\right|. \tag{16}$$

Hence, $I_m(H)$ can be evaluated numerically; a good approximation for $I_m(H)$ can be obtained as follows.

The odd function $\varphi_0(\mu)$ can be written as the Fourier series $\Sigma a_n \sin(2n+1)\mu$ to satisfy the boundary condition (11). We take the lowest approximant $\varphi_0 = a_0\sin\mu$ with $a_0 = 0.43$ to fit the difference $\varphi_0(w) - \varphi_0(0) = 0.86$ that is found

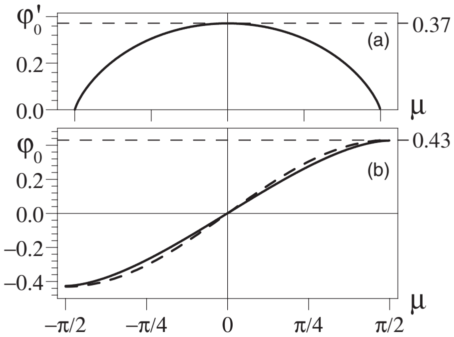

FIG. 2. (a) The function $\varphi_0'(\mu)$ calculated according to Eq. (14). (b) The solid line is $\varphi_0(\mu)$ obtained by numerical integration of $\varphi_0'(\mu)$ shown in the panel (a). The dashed line is the approximation $\varphi_0(\mu)=0.43\sin\mu$.

integrating numerically the exact derivative in Eq. (14). The comparison of the phase found numerically with $a_0\sin\mu$ is shown in Fig. 2(b).

In this approximation we have

$$\frac{I_m}{g_c w}=\frac{1}{\pi}\left|\int_{-\pi/2}^{\pi/2}d\mu\,\cos(ha_0\sin\mu)\right|=|J_0(a_0h)|. \quad (17)$$

Figure 3 shows that this approximation is quite accurate as compared to $I_m(H)$ calculated numerically with the help of Eq. (16). Zeros of the Bessel function $J_0(x)$ are equidistant for large arguments, but they are spaced roughly by π everywhere. Hence zeros of $I_m(h)$ are separated by $a_0\Delta h\simeq\pi$, or in common units by

$$\Delta H\simeq 1.8\phi_0/w^2. \quad (18)$$

It is worth recalling that in bulk junctions of the length w the zeros are separated by $\Delta H\approx 2\phi_0/w\lambda$ that exceeds by much the thin-film spacing. A similar estimate is given in Ref. 10.

In the high-field region one can use the large argument asymptotics of $J_0(x)$ to obtain

$$I_m\approx 0.61g_c\sqrt{\frac{\phi_0}{H}}\left|\cos\left(1.72\frac{Hw^2}{\phi_0}-\frac{\pi}{4}\right)\right|. \quad (19)$$

Thus, the maxima of $I_m(H)$ decrease as $1/\sqrt{H}$, i.e., slower than in the bulk case where $I_m\propto 1/H$.

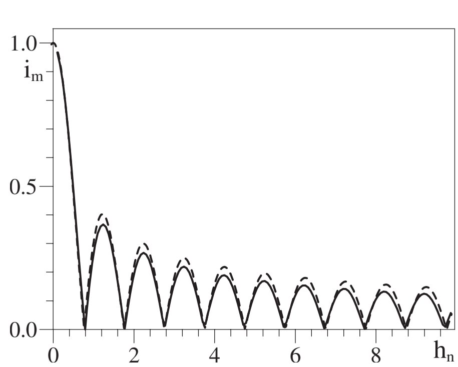

FIG. 3. The maximum supercurrent $i_m=I_m/g_cw$ versus the normalized applied field $h_n=4a_0w^2H/\pi\phi_0$. The dashed line is the approximation (17).

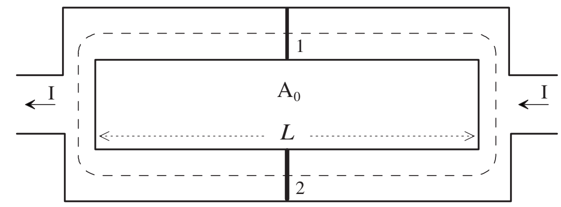

FIG. 4. Sketch of a rectangular SQUID made of two narrow thin-film strips with identical edge-type junctions 1 and 2.

It is worth noting that in high fields the maxima $I_m(H)$ do not depend on the junction length w. Qualitatively, this comes about because the tunneling current $g_x=g_c\sin(h\varphi_0+\theta)$ oscillates fast for $h\gg 1$ so that most of the junction length does not contribute to the total current, unlike the narrow belts of the width $\delta\sim\sqrt{\phi_0/H}$ near the strip edges.

In practice the pattern shown in Fig. 3 might be distorted by Pearl vortices trapped in the junction banks. The energy of these vortices acquires a minimum in the strip middle starting from fields of the order ϕ_0/w^2.[19–22] However, estimates of the energy ϵ_J of Josephson vortices as compared to Pearl ones, ϵ_P, yield $\epsilon_J/\epsilon_P\sim 0.1/\ln(2w/\xi)$, where ξ is the coherence length and $\ln(2w/\xi)$ is large. Physically, this makes the Josephson contact a "weak spot" where vortices penetrate the sample first. Hence the chances are good for recording quite a few maxima of $I_m(H)$ provided the strip is homogeneous and the pinning is weak.

Let us consider now current flowing through rectangular SQUID made of narrow thin-film strips with two identical junctions sketched in Fig. 4. In zero field the current distribution is symmetric with respect to the SQUID center and the line integral of $\boldsymbol{g}$ along any symmetric contour is zero. When the field is applied, this symmetry is violated by the screening currents. However, at the contour in the strip middle (shown in the figure) the screening currents vanish so that the contour integral of $\boldsymbol{g}$ remains zero. This contour crosses the junctions at their middle. The flux ϕ enclosed by this contour does not change if the contour is shifted as a whole by μ. Integrating the London equation for $\mathbf{g}$ over such a contour we obtain

$$\varphi_2(\mu)-\varphi_1(\mu)=2\pi\phi/\phi_0. \quad (20)$$

The total current through the system is given by

$$\begin{aligned}\frac{\pi I}{g_cw}&=\int_{-\pi/2}^{\pi/2}d\mu(\sin\varphi_1+\sin\varphi_2)\\&=2\int_{-\pi/2}^{\pi/2}d\mu\,\sin\left(ha_0\sin\mu+\theta+\frac{\pi\phi}{\phi_0}\right)\cos\left(\frac{\pi\phi}{\phi_0}\right),\end{aligned} \quad (21)$$

where θ is a constant. The maximum current corresponds to $\theta=\pi/2-\pi\phi/\phi_0$:

$$I_m=2g_cw\left|J_0\left(4a_0\frac{w^2}{A_0}\frac{\phi}{\phi_0}\right)\cos\left(\pi\frac{\phi}{\phi_0}\right)\right|, \quad (22)$$

where A_0 is the area of the "central" contour. Note that Eq. (22) is valid if $L\gg w$ (see Fig. 4).

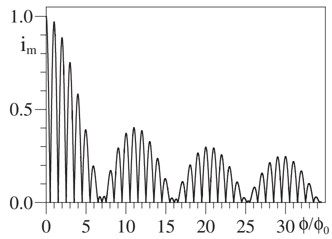

FIG. 5. The maximum supercurrent $i_m = I_m/2g_c w$ versus flux ϕ/ϕ_0 for a rectangular SQUID (Fig. 4) with $A_0/w^2=5$.

An example of $I_m(\phi/\phi_0)$ is shown in Fig. 5 for a SQUID with $A_0/w^2=5$. The standard SQUID pattern $|\cos(\pi\phi/\phi_0)|$ is modulated in our case by a slow varying Bessel function. We stress again that the pattern shown is obtained for large area SQUIDs with two narrow thin-film junctions; for reduced areas the interference patterns become more complex, a subject for further study.

To summarize, we have evaluated the field dependence of the maximum supercurrent in narrow edge-type Josephson junctions in thin-film strips; the strip width w is supposed to be less than the Pearl length Λ and the thin-film Josephson length ℓ of Eq. (1). Calculations are done in the framework of nonlocal Josephson electrodynamics. We demonstrate that the stray fields cause a pattern $I_m(H)$ with much reduced distance between zeros, $\Delta H \sim \phi_0/w^2$, and with a slow decreasing maxima in high fields, $I_m(H) \propto 1/\sqrt{H}$. The flux dependence of the maximum supercurrent through a SQUID made of narrow thin-film strips with edge-type junctions differs by much from the standard periodicity.

The authors are grateful to J. Mannhart, C. Schneider, and A. Gurevich for stimulating discussions. The work of V.G.K. at Ames Laboratory was supported by the Office of Basic Energy Sciences of the U.S. Department of Energy under Contract No. DE-AC02-07CH11358.

*mints@post.tau.ac.il

[1] Y. M. Ivanchenko and T. K. Soboleva, Phys. Lett. A **147**, 65 (1990); Y. M. Ivanchenko, Phys. Rev. B **52**, 79 (1995).
[2] A. Gurevich, Phys. Rev. B **46**, 3187 (1992).
[3] R. G. Mints and I. B. Snapiro, Phys. Rev. B **49**, 6188 (1994); **51**, 3054 (1995); **52**, 9691 (1995).
[4] Y. E. Kuzovlev and A. I. Lomtev, Sov. Phys. JETP **84**, 986 (1997).
[5] V. G. Kogan, V. V. Dobrovitski, J. R. Clem, Y. Mawatari, and R. G. Mints, Phys. Rev. B **63**, 144501 (2001).
[6] D. J. Van Harlingen, Rev. Mod. Phys. **67**, 515 (1995).
[7] C. C. Tsuei and J. R. Kirtley, Rev. Mod. Phys. **72**, 969 (2000).
[8] H. Hilgenkamp and J. Mannhart, Rev. Mod. Phys. **74**, 485 (2002).
[9] A. A. Abdumalikov, Jr., M. V. Fistul, and A. V. Ustinov, Phys. Rev. B **72**, 144526 (2005).
[10] P. A. Rosenthal, M. R. Beasley, K. Char, M. S. Colclough, and G. Zaharchuk, Appl. Phys. Lett. **59**, 3482 (1991).
[11] R. G. Mints, Phys. Rev. B **57**, R3221 (1998).
[12] R. G. Mints, I. Papiashvili, J. R. Kirtley, H. Hilgenkamp, G. Hammerl, and J. Mannhart, Phys. Rev. Lett. **89**, 067004 (2002).
[13] S. M. Frolov, D. J. Van Harlingen, V. V. Bolginov, V. A. Oboznov, and V. V. Ryazanov, Phys. Rev. B **74**, 020503(R) (2006).
[14] M. Weides, M. Kemmler, E. Goldobin, H. Kohlstedt, R. Waser, D. Koelle, and R. Kleiner, Phys. Rev. Lett. **97**, 247001 (2006).
[15] J. Mannhart, H. Hilgenkamp, B. Mayer, C. Gerber, J. R. Kirtley, K. A. Moler, and M. Sigrist, Phys. Rev. Lett. **77**, 2782 (1996).
[16] H. J. H. Smilde, Ariando, D. H. A. Blank, G. J. Gerritsma, H. Hilgenkamp, and H. Rogalla, Phys. Rev. Lett. **88**, 057004 (2002).
[17] A. Barone and G. Paterno, *Physics and Applications of the Josephson Effect* (Wiley, New York, 1982).
[18] E. H. Brandt, Phys. Rev. B **46**, 8628 (1992).
[19] V. G. Kogan, J. R. Clem, and R. G. Mints, Phys. Rev. B **69**, 064516 (2004).
[20] G. Stan, S. B. Field, and J. M. Martinis, Phys. Rev. Lett. **92**, 097003 (2004).
[21] E. Bronson, M. P. Gelfand, and S. B. Field, Phys. Rev. B **73**, 144501 (2006).
[22] K. H. Kuit, J. R. Kirtley, W. van der Veur, C. G. Molenaar, F. J. G. Roesthuis, A. G. P. Troeman, J. R. Clem, H. Hilgenkamp, H. Rogalla, and J. Flokstra, Phys. Rev. B **77**, 134504 (2008).